International Refereed Journal of Engineering and Science (IRJES)
ISSN (Online) 2319-183X, (Print) 2319-1821
Volume 5, Issue 10 (October 2016), PP.18-27

An Analysis and Reduction of Fractional Brownian motion Noise in Biomedical Images Using Curvelet Transform and Various Filtering and Thresholding Techniques

[1]S.Vanitha, [2]R.Rajeswari and [3]D.Ebenezer
[1]*Assistant Professor (Senior Grade), Department Of ECE, PSG Institute Of Technology And Applied Research, Coimbatore, Tamilnadu, India.*
[2]*Associate Professor, Department Of EEE, Government College Of Technology Coimbatore, Tamilnadu, India.*
[3]*Professor, Department Of ECE, Easwari Engineering College, Chennai, Tamilnadu, India.*

Abstract: The application of image restoration is not limited to the case of medical images especially in case of high resolution brain MRI images. The fractional Brownian motion noise present in these images affects certain important features which are needed for the proper diagnosis of brain diseases. Removal of fBm noise in these images is a kind of difficulty the researcher experiences. This paper investigates the various noise reduction techniques for reducing the fractional Brownian motion noise by using curvelet transform, various filtering techniques such as bilateral filter, trilateral filter, thresholding techniques like VisuShrink, NeighShrink and BayesShrink. The performance of all these techniques is analyzed using PSNR (Peak Signal to Noise Ratio), SSIM (Structural Similarity Index Metric), FD (Fractal Dimension), IEF (Image Enhancement Factor) and time elapsed. The performance of discrete curvelet transform, NeighShrinkand VisuShrink methods are found to be similar and relatively better than other techniques in terms of PSNR and SSIM. But curvelet transform requires increased computation time than other noise reduction techniques.

I. INTRODUCTION

Noise suppression in medical images is a tantalizing and challenging job. The diagnostically related image content can be enhanced by a tradeoff between noise reduction and the preservation of actual image features. While acquiring or transmitting images, images are corrupted by various types of noise. The retention of the most potential features of the image can be achieved by eliminating the noise i.e. denoising and this should be the objective of denoising. Among medical images, tumor images in brain have high degree of randomness accompanied with natural random structure.

Mandelbrot used the term fractal from Latin and developed Fractal concept. Mandelbrot and Van Ness [1] [2] explained the complex geometry of the objects in nature by fractal concept. A fractal is an irregular geometric object with an infinite nesting of structure at all scales .One of the applications of fractals is modeling random signals. The authors have developed a fractional Brownian model for tumor [18]. A related application is fractional Brownian noise. In this paper performance of thresholding techniques like BayeShrink, NeighShrink, Visushrink, filtering methods like bilateral and trilateral filters and curvelet transform method are analyzed for reduction of fractional Brownian motion noise.

The work on signal denoising via wavelet thresholding or shrinkage of Donoho & Johnstone [3]-[5] have shown that various wavelet thresholding schemes for denoising have near optimal properties in the mini-max sense and perform well in simulation studies of one dimensional curve estimation. The wavelet thresholding methods have rates of convergence better than linear methods for approximating functions in Besov spaces [3] [4]. Thresholding is a nonlinear technique, which is very simple as it operates on one wavelet coefficient at a time.

Various biomedical image processing applications imply filtering as a preliminary process. Image processing tasks such as segmentation and classification follow noise filtering.

II. BACKGROUND STUDY

The concept of bilateral filtering for edge-preserving smoothing was proposed by Tomasi & Manduchi [6] in which bilateral filtering is formulated as combination of domain filtering and range filtering. Bilateral filtering smooths images while preserving edges, by means of a nonlinear combination of nearby image values. The method is non-iterative, local and simple. The output image of low pass domain filter is characterized by,

$$h(x) = k_d^{-1}(x) \int_{-\infty}^{\infty} \int_{-\infty}^{\infty} f(\xi) c(\xi, x) d\xi \quad (1)$$

where $c(\xi, x)$ measures the geometric closeness between the neighborhood center **x** and a nearby point ξ

.

Range filtering is defined as,

$$h(x) = k_r^{-1}(x) \int_{-\infty}^{\infty} \int_{-\infty}^{\infty} f(\xi) s(f(\xi), f(x)) d\xi \quad (2)$$

The combined filtering is expressed as,

$$h(x) = k^{-1}(x) \int_{-\infty}^{\infty} \int_{-\infty}^{\infty} f(\xi) c(\xi, x) s(f(\xi), f(x)) d\xi \quad (3)$$

with the normalization $k(x) = \int_{-\infty}^{\infty} \int_{-\infty}^{\infty} c(\xi, x) s(f(\xi), f(x)) d\xi$ (4)

Trilateral filter which can achieve edge-preserving smoothing with a narrow spatial window in only a few iterations was proposed by Wong et al[7]. It has greater noise reduction capability than bilateral filtering and smooths the biomedical images without over – smoothing ridges and shifting the edge locations.

The smoothing and edge preserving is achieved to a satisfactory extent by the implementation of trilateral filter in preference to bilateral filter. The discrete form of bilateral filter is given as

$$\vec{I}^*(\vec{x}) = \frac{1}{k(\vec{x})} \sum_{\vec{\xi} \epsilon \mathcal{N}_{\vec{x}}} \vec{I}(\vec{\xi}). c(\vec{\xi}, \vec{x}). s(\vec{I}(\vec{\xi}), \vec{I}(\vec{x})) \quad (5)$$

where $\vec{x}$ and $\vec{\xi}$ are spatial coordinates, $\vec{I}$ is the noisy image and $\vec{I}^*$ is the filtered image. $\mathcal{N}_{\vec{x}}$ defines the spatial window around the pixel at $\vec{x}$.

Similarly trilateral filter can be expressed as

$$\vec{I}^{(t+1)}(\vec{x}) = \frac{1}{k(\vec{x})} \sum_{\vec{\xi} \epsilon \mathcal{N}_{\vec{x}}} \vec{I}^{(t)}(\vec{\xi}). \omega(\vec{\xi}, \vec{x}, t) \quad (6)$$

where

$$\omega(\vec{\xi}, \vec{x}, t) = (1 - a(\vec{x})). c(\vec{\xi}, \vec{x}) + a(\vec{x}). c(\vec{\xi}, \vec{x}). s\left(\vec{I}^{(t)}(\vec{\xi}), \vec{I}^{(t)}(\vec{x})\right). \sum_{i=1}^{p-1} d_i(\vec{\xi}, \vec{x}) \quad (7)$$

Local structural information can be extracted from the images; normalized local signal amplitude is given as,

$$a(\vec{x}) = m(A^*_{\vec{x}}, p, q) = \frac{(A^*_{\vec{x}}.(1-p))^q}{(A^*_{\vec{x}}.(1-p))^q + ((1-A^*_{\vec{x}}).p)^q} \quad (8)$$

where m is the mapping function, p ϵ [0, 1] and q are positive constants.

VisuShrink was proposed by Donoho & Johnstone [8]. The expression for universal threshold is $T_U = \sigma\sqrt{2\log M}$. Here M represents the signal length and σ is the noise variance. It uses a threshold value that is proportional to the standard deviation of the noise. It follows the hard threshold rule. An estimate of the noise level σ was defined based on the median absolute deviation given by

$$\bar{\sigma} = \frac{Median(\{|g_{j-1,k}| : k = 0, 1, \ldots, 2^{j-1} - 1\}}{0.6745} \quad (9)$$

where $g_{j-1,k}$ are the detailed coefficients in the wavelet transform.

An adaptive data - driven threshold for image denoising via soft – thresholding known as BayesShrink was proposed by Chang et al [9]. The threshold is derived in a Bayesian framework, and the prior used on the wavelet coefficients is the generalized Gaussian distribution (GGD) widely used in image processing applications. The proposed threshold is simple and closed-form, and itis adaptive to each subband because it depends on data-driven estimates of the parameters. Soft and hard thresholding are the two thresholding methods which are used in common. The soft-thresholding function is given as,

$$\eta_T(x) = \text{sgn}(x).\max(|x| - T, 0) \quad (10)$$

The hard-thresholding function is given as,

$$\psi_T(x) = x.1\{|x| > T\} \quad (11)$$

The Generalized Gaussian Distribution is given as,

$$GG_{\sigma X,\beta}(x) = C(\sigma_x, \beta)\exp\{-[\alpha(\sigma_x, \beta)|x|^{\beta}\} \quad -\infty < x < \infty, \sigma_x > 0, \beta > 0 \quad (12)$$

$$where \quad \alpha_x(\sigma_x, \beta) = \sigma_x^{-1}\left[\frac{\Gamma(\frac{3}{\beta})}{\Gamma(\frac{1}{\beta})}\right]^{1/2}, C(\sigma_x, \beta) = \frac{\beta.\alpha(\sigma_x, \beta)}{2\Gamma(\frac{1}{\beta})}$$

and $\Gamma(t) = \int_0^{\infty} e^{-u} u^{t-1} du$ is the gamma function.

The parameter σ_x is the standard deviation and β is the shape parameter. For a given set of parameters, the objective is to find a soft – threshold T which minimizes the Bayes risk.

The digital implementation of ridgelet and curvelet transforms was presented by Starck et al[10]. The discrete curvelet transform algorithm was proposed as below:

1) apply the à trous algorithm with J scales;
2) set $B_1 = B_{min}$;
3) for j = 1,…..J do

a) partition the subbandw_j with a block size $B_j$and apply the digital ridgelet transform to each block
b) if j modulo2 = 1 then $B_{j+1} = 2\ B_j$

c) else $B_{j+1} = B_j$.

The sidelength of the localizing windows are doubled at every other dyadic subband, hence maintaining the fundamental property of the curvelet transform, which says that elements of length about $2^{-j/2}$ serve for the analysis and synthesis of the j^{th} subband $[2^j, 2^{j+1}]$.It was observed that the curvelet transform is superior to local ridgelet transforms, regardless of the block size. The curvelet reconstruction does not have disturbing artifacts along edges and also highly sensitive in comparison with wavelet – based reconstructions.

Image denoising using neighbouring wavelet coefficients (NeighShrink) was proposed by Chen et al [11]. Assuming $d_{j,k}$ as set of wavelet coefficients of the noisy 1D signal, the thresholding formula is given as

$$d_{j,k} = d_{j,k}\beta_{j,k} \quad (13)$$

where the shrinkage factor is defined as

$$\beta_{j,k} = \left(\frac{1-\lambda^2}{s_{j,k}^2}\right)_+ \quad (14)$$

The + sign at the end of the formula implies $\beta_{j,k}$ is positive, where λ is given as

$$\lambda = \sqrt{2\sigma^2 \log n^2} \quad (15)$$

where n is the length of signal.

III. FRACTIONAL BROWNIAN MOTION NOISE

Noise is undesired information that degrades the image. In the image de-noising process, information of the type of noise present in the original image plays a significant role. Brownian noise is under the category of fractal or 1/f noise. The mathematical model for 1/f noise is the fractional Brownian motion. Brownian motion is non-stationary stochastic process which follows a normal distribution. Brownian noise is a special case of 1/f noise. It can be obtained by integrating white noise.

Fractional Brownian motion and its properties

Mandelbrot and Van Ness [1] had carried out the ground-breaking work which expresses stochastic representation of fBm

$$B_H(t) = \frac{1}{\Gamma\left(H+\frac{1}{2}\right)}\left(\int_{-\infty}^{0}\left[(t-s)^{H-\frac{1}{2}} - (-s)^{H-\frac{1}{2}}\right]dB(s) + \int_0^t (t-s)^{H-\frac{1}{2}}dB(s)\right) \quad (16)$$

where Γ represents the Gaussian function

$$\Gamma(\alpha) = \int_0^\infty x^{\alpha-1}exp(-x)dx \quad (17)$$

Yaglom [12] described the non-stationary property of fBm in terms of covariance structure

$$E[B_H(t)B_H(s)] = \frac{\sigma^2}{2}(|t|^{2H} + |s|^{2H} - |t-s|^{2H}) \quad (18)$$

where $H \in (0,1)$ called the Hurst parameter or fractal parameter. The fractal parameter is related to the dynamic behavior of the fBm, and when H = ½, fBm is the well-known classical Brownian motion. The variance of the fBm is of the type [13]

$$var(B_H(t)) = \sigma^2|t|^{2H} \quad (19)$$

The fractal dimension is given by [2] [14]

D = 2 – H

According to the possible values of H, it follows that 1 < D < 2, the scalar fBm parameter H being related to the roughness of fBm samples.

A normalized fractional Brownian motion $B_H = \{B_H(t): 0 \leq t < \infty\}$ with 0 < H < 1 is uniquely characterized by the following properties [15]

1. $B_H(t)$ has stationary increments
2. $B_H(0) = 0\ \&\ EB_H(t) = 0\ ;\ for\ all\ t$

3. $EB^2{}_H(t) = t^{2H}; for\ all\ t$
4. $B_H(t)$ has a Gaussian distribution for $t > 0$.

The wavelet representation of fBm[16]

$$B_H(t) - b_0 = \sum_k b_h(k)\phi_{0,k}^{(s)}(t) + \sum_{j\le 0,k} \gamma_j(k)\, 4^{-s} 2^{-js} \psi_{j,k}^{(s)}(t) \quad (20)$$

where $s = H + \frac{1}{2}$, b_0 is an arbitrary constant, γ_j are independent identically distributed Gaussian random variables, $b_h(k)$ is a fractional $ARIMA(0, s, 0)$ process, and $\phi_{0,k}^{(s)}$ and $\psi_{j,k}^{(s)}$ are suitably defined fractional scaling function and wavelet.

Simulation of fractional Brownian motion noise

Fractional Brownian motion noise is generated by random displacement method proposed by PenttinenVirtamo[17].The two dimensional fractional Brownian motion noise is as shown in figure 1 for Hurst parameter H = 0.3 and H = 0.7.

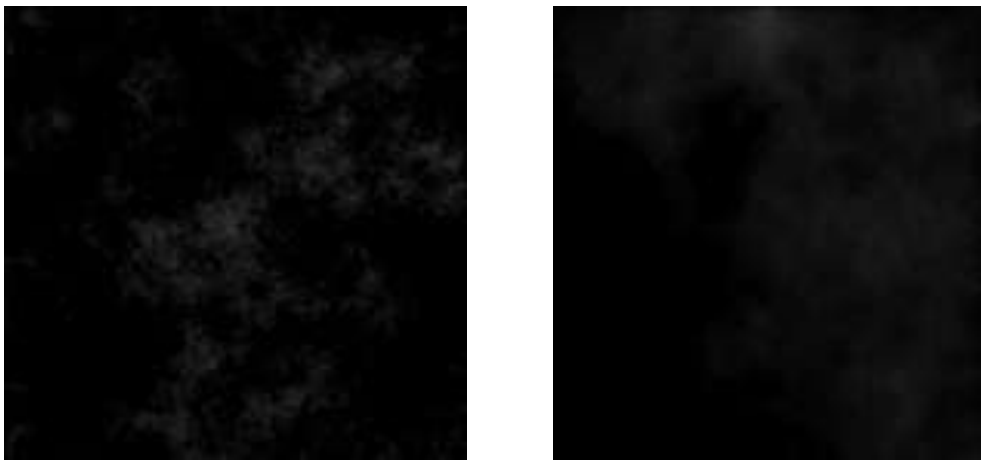

(a) **(b)**

Figure 1 (a) fBmnoise with H = 0.3 and (b) H =0.7

IV. Experimental results and discussion

The fractional Brownian motion noise is added to brain MRI images shown in figure 2. The performance of the de-noising methods is analyzed using the performance metrics like peak signal to noise ratio(PSNR),structural similarity index metric (SSIM),image enhancement factor(IEF),fractal dimension(FD) and time elapsed. The fBm noise is added to normal brain MRI image, MRI image with low grade and with modeled tumor [18]. The input MRI images without fBm noise are shown in figure 2.

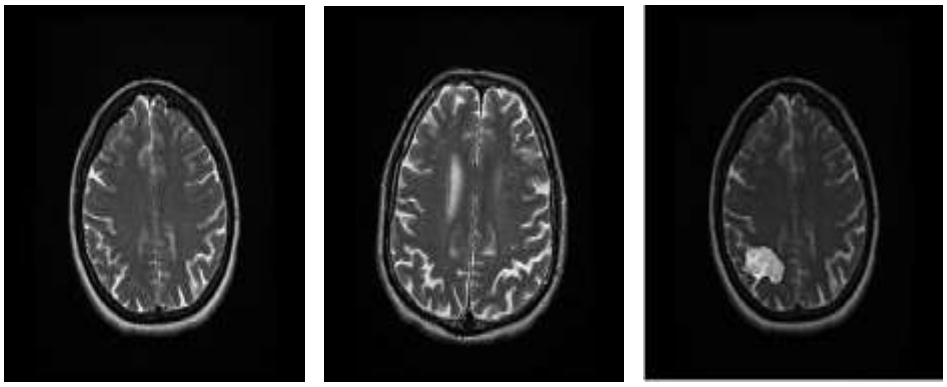

(a) **(b)** **(c)**

Figure 2 (a) fBmnoise with H = 0.3 and (b) H =0.7

The input images with fBm noise with H = 0.3 and H = 0.7 are shown in figure 3. Filtering methods, namely bilateral and trilateral filters are used for denoising the fractional Brownian noise with H = 0.3 and H = 0.7.The corresponding output images are shown in figures4 and 5.The output images for thresholding

techniques, namely BayesShrink, NeighShrink, VisuShrink soft and hard thresholding are shown in figures 6, 7, 8 and 9 respectively .The output images for Curvelet transform are shown in figure 10.

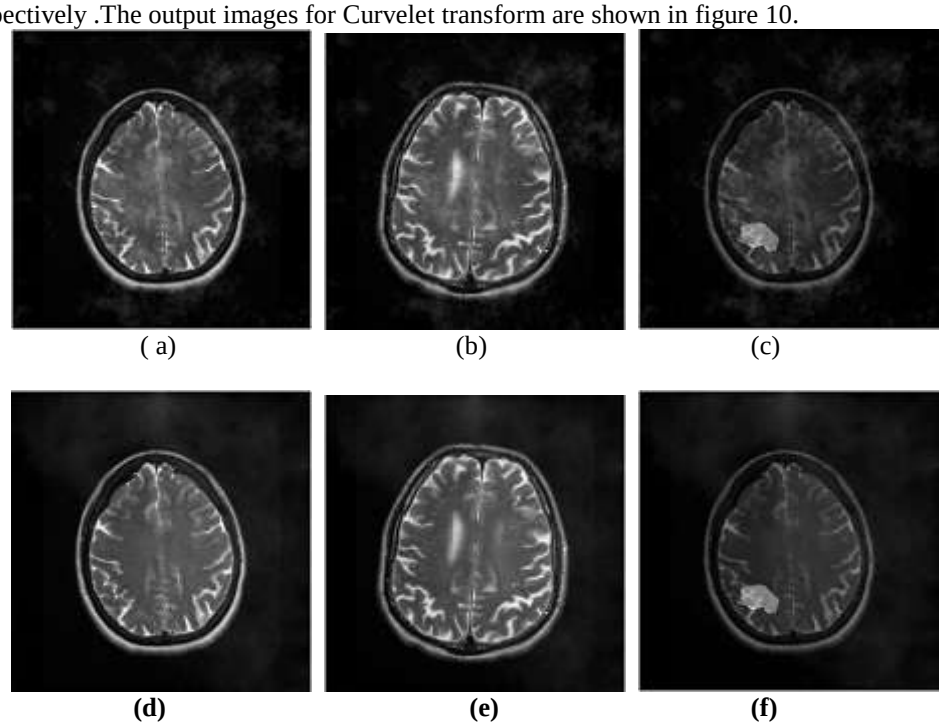

(a) (b) (c)

(d) (e) (f)

Figure 3 (a) fBm noise with H = 0.3 in normal brain MRI image (b) with low grade tumor (c) modeled tumor (d) fBm noise with H = 0.7 in normal brain MRI image (e) with low grade tumor (f) modeled tumor

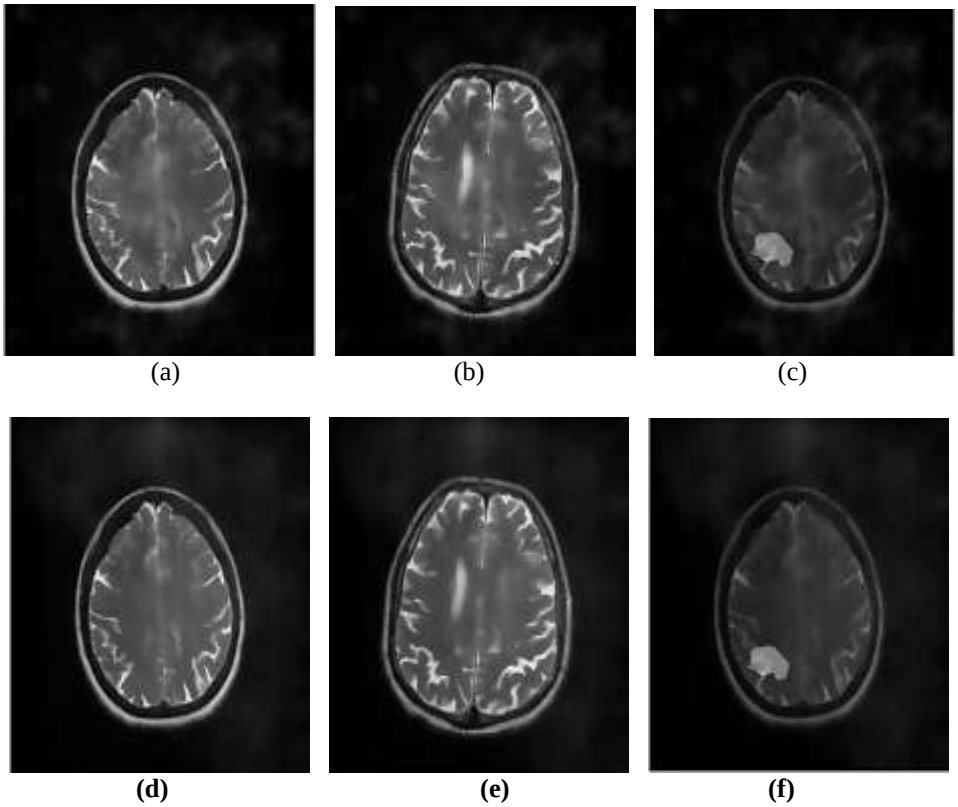

(a) (b) (c)

(d) (e) (f)

Figure 4 Output image for (a) bilateral filtering for fBm noise with H = 0.3 in normal brain MRI image (b) with low grade tumor (c) modeled tumor and (d) for fBm noise with H = 0.7 in normal brain MRI image (e)low grade tumor (f) modeled tumor

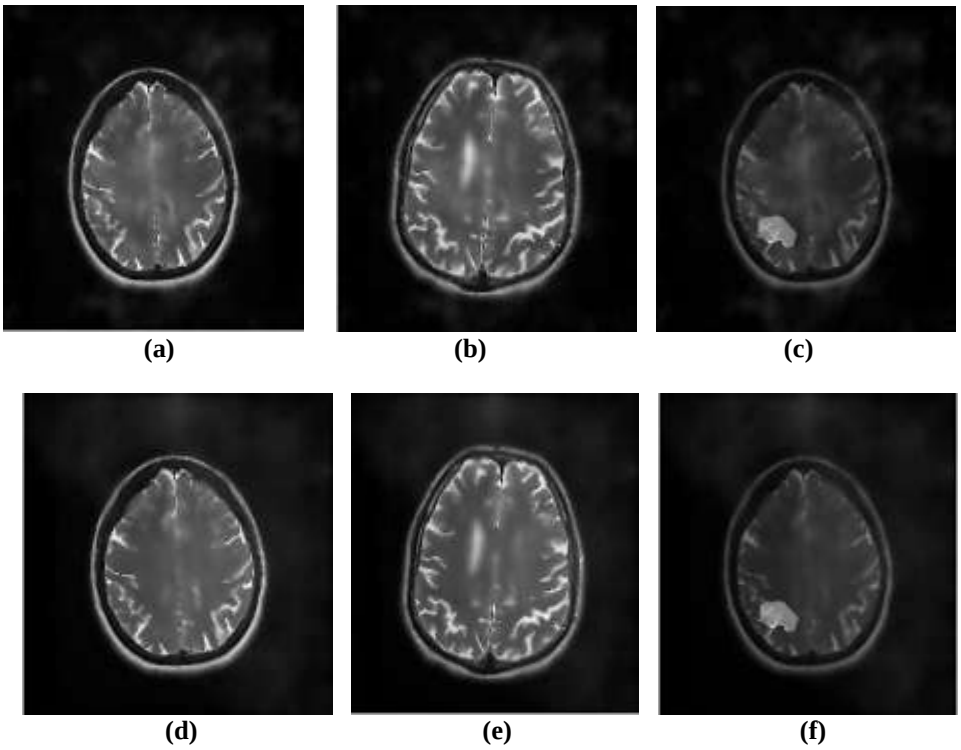

Figure5 Output image for (a) trilateral filtering for fBm noise with H = 0.3 in normal brain MRI image (b) with low grade tumor (c) modeled tumor and (d) for fBm noise with H = 0.7 in normal brain MRI image (e)low grade tumor (f) modeled tumor

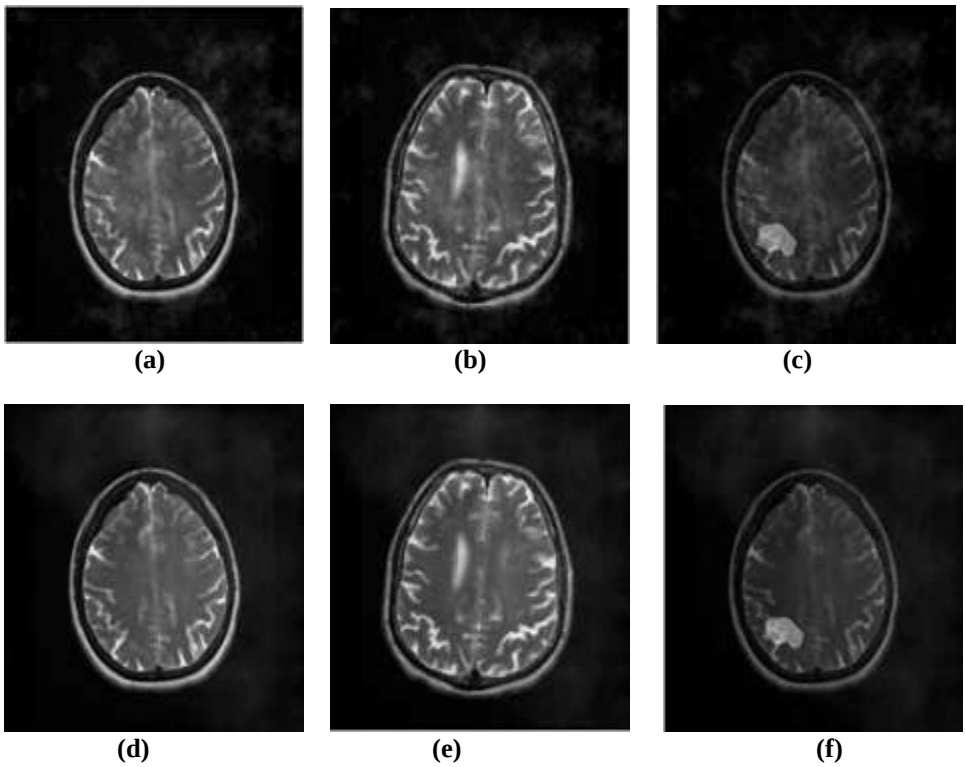

Figure6 Output image for (a) BayesShrink for fBm noise with H = 0.3 in normal brain MRI image (b) with low grade tumor (c) modeled tumor and (d) for fBm noise with H = 0.7 in normal brain MRI image (e)low grade tumor (f) modeled tumor

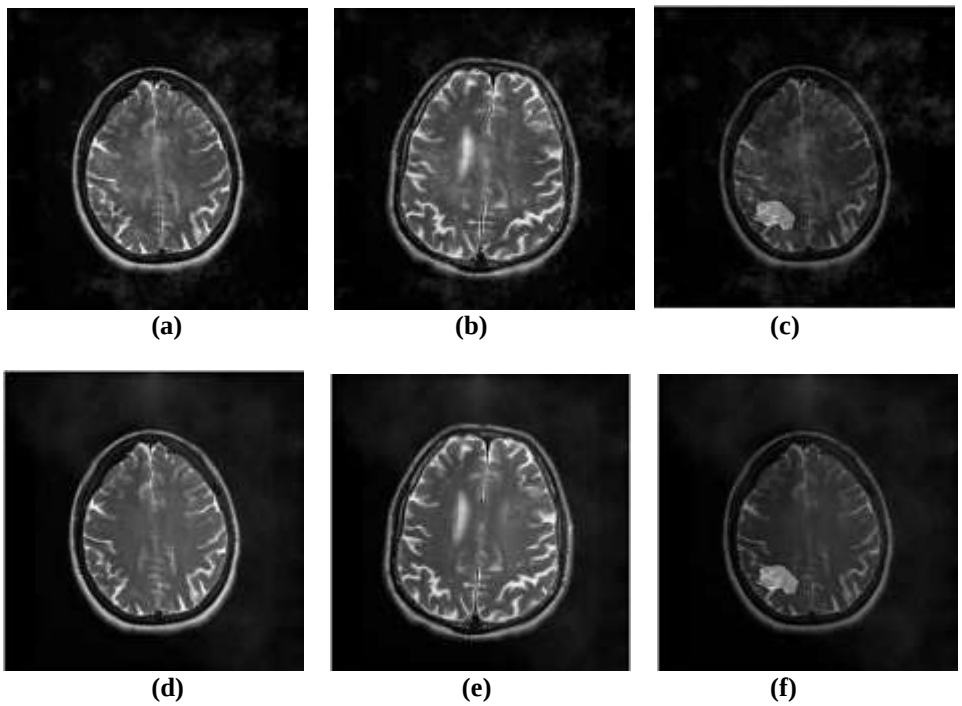

(a) **(b)** **(c)**

(d) **(e)** **(f)**

Figure7 Output image for (a) NeighShrink for fBm noise with H = 0.3 in normal brain MRI image(b) with low grade tumor (c) modeled tumor and (d) for fBm noise with H = 0.7 in normal brain MRI image (e)low grade tumor (f) modeled tumor

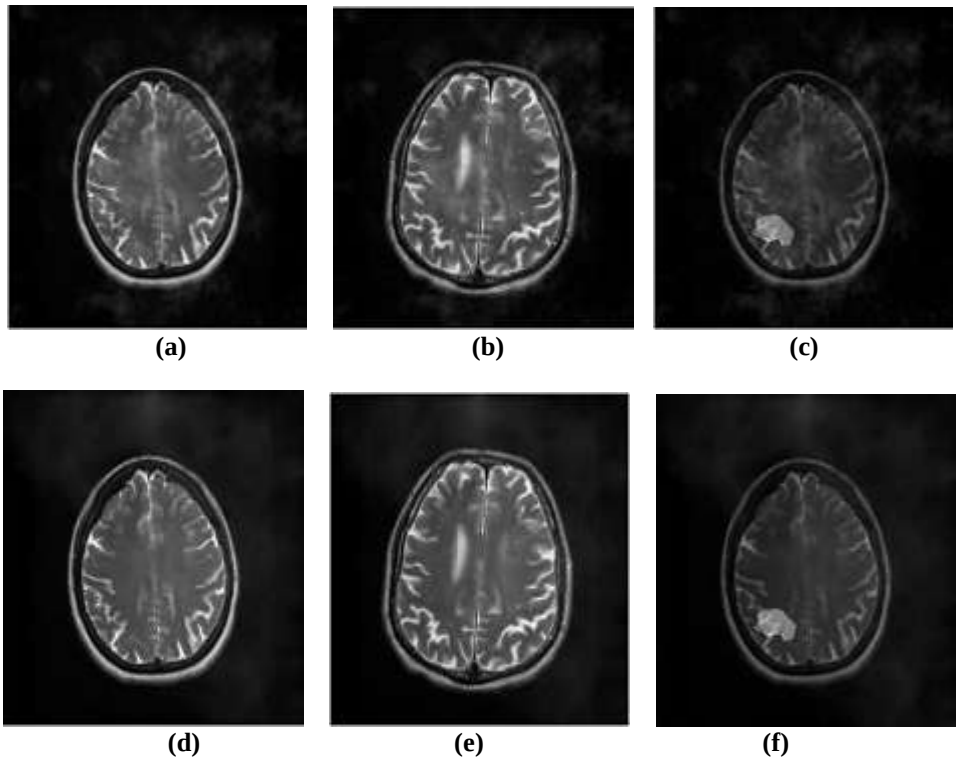

(a) **(b)** **(c)**

(d) **(e)** **(f)**

Figure8 Output image for (a) Visu Soft thresholding method for fBm noise with H = 0.3 in normal brain MRI image (b) with low grade tumor (c) modeled tumor and (d) for fBm noise with H = 0.7 in normal brain MRI image (e) low grade tumor (f) modeled tumor

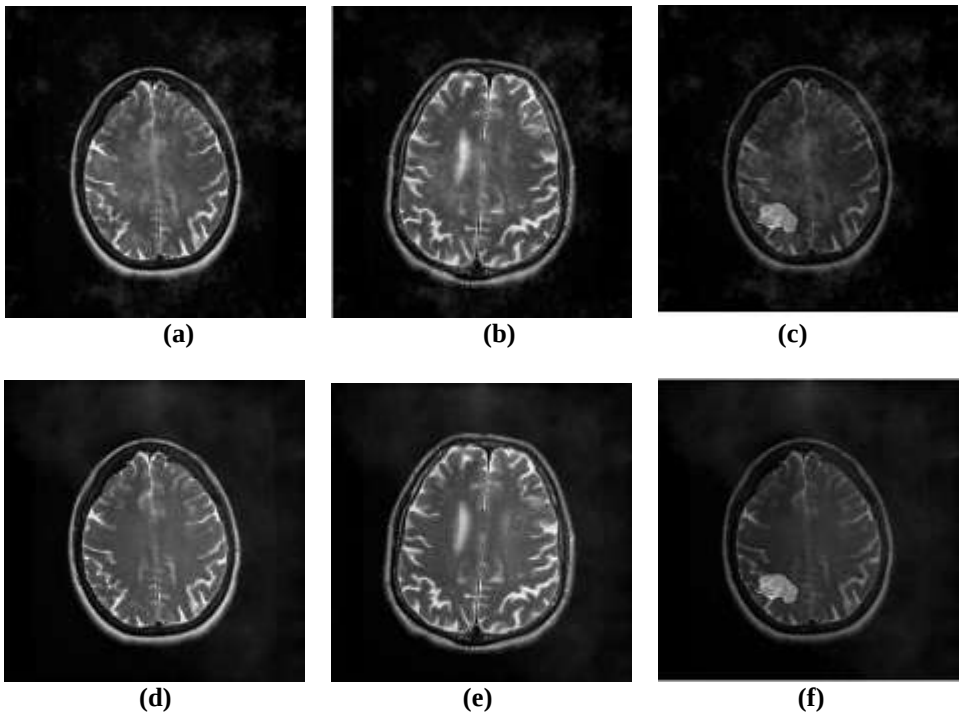

Figure9 Output image for (a) Visu Hard thresholding method for fBm noise with H = 0.3 in normal brain MRI image (b) with low grade tumor (c) modeled tumor and (d) for fBm noise with H = 0.7 in normal brain MRI image (e)low grade tumor (f) modeled tumor.

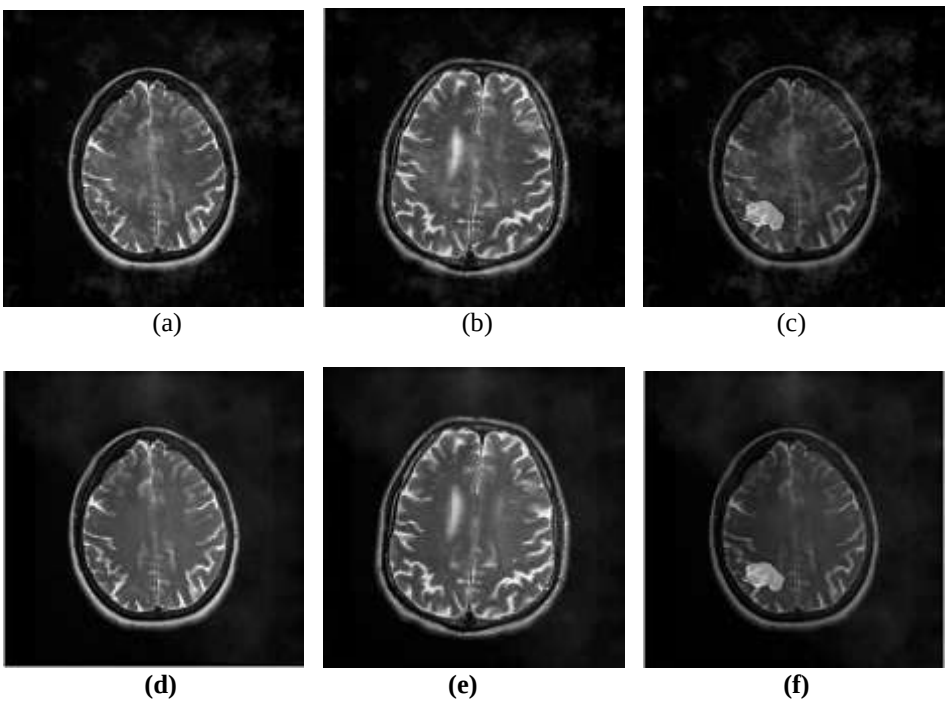

Figure10 Output image for (a) Curvelet transform denoising method for fBm noise with H = 0.3 in normal brain MRI image (b) with low grade tumor (c) modeled tumor and (d) for fBm noise with H = 0.7 in normal brain MRI image (e)low grade tumor (f) modeled tumor

The curvelet transform is better than other methods based on PSNR for all types of MRI images, but the fBm noise is not removed completely. The time elapsed for curvelet transform is higher than other noise reduction methods. The performance of various noise reduction techniques are compared for fBm noise alone with H = 0.3 and H = 0.7 are shown in table 1 and 2 respectively.

Table 1 Comparison of various noise reduction techniques for fBm noise with H = 0.3

S.No.	Parameters		BS	NS	BF	DCT	TF	VS	
								Soft	Hard
1	PSNR	Normal	27.7537	28.1360	14.4625	28.2806	27.3498	28.1821	28.0629
		Low grade	27.4037	28.1223	13.0763	28.2010	26.8113	28.0912	28.0848
		Modeled	28.1671	28.1615	19.5543	28.2981	28.0052	28.2978	28.0800
2	SSIM	Normal	0.8033	0.8082	0.4078	0.8078	0.7884	0.8014	0.7994
		Low grade	0.7949	0.8102	0.4040	0.8107	0.8009	0.8160	0.8007
		Modeled	0.7706	0.7661	0.5290	0.7627	0.7536	0.7627	0.7570
3	IEF	Normal	0.9343	1.0203	0.0438	1.0171	0.8513	1.0312	1.0032
		Low grade	0.8620	1.0171	0.0318	1.0174	0.7521	1.0098	0.9992
		Modeled	1.0276	1.0263	0.1414	1.0157	0.9900	1.0590	1.0072
4	FD	Normal	1.9509	1.9384	2.0000	1.9325	1.9564	1.9406	1.9305
		Low grade	1.9339	1.9181	2.0000	1.9077	1.9402	1.9195	1.9098
		Modeled	1.9843	1.9786	2.0000	1.9765	1.9853	1.9796	1.9762
5	Time Elapsed in Seconds	Normal	0.3299	2.5547	2.7544	76.3439	135.726	0.1631	0.3139
		Low grade	0.3290	2.5645	2.6992	76.8033	134.858	0.1761	0.3281
		Modeled	0.3209	2.5464	2.9023	76.8180	142.479	0.1791	0.3138

Table 2 Comparison of various noise Reduction techniques for fBm noise with H = 0.7

S.No.	Parameters		BS	NS	BF	DCT	TF	VS	
								Soft	Hard
1	PSNR	Normal	25.3437	25.5903	14.4629	25.6134	24.9096	25.5816	25.6026
		Low grade	25.1544	25.5872	13.0768	25.6141	24.5733	25.5669	25.6016
		Modeled	25.5644	25.5977	19.5549	25.6149	25.2692	25.6065	25.6077
2	SSIM	Normal	0.6864	0.7028	0.4102	0.7121	0.6597	0.7037	0.7078
		Low grade	0.6976	0.7185	0.4036	0.7255	0.6703	0.7181	0.7220
		Modeled	0.6409	0.6503	0.5312	0.6570	0.6099	0.6519	0.6542
3	IEF	Normal	0.9403	0.9953	0.0768	1.0006	0.8509	0.9933	0.9981
		Low grade	0.9002	0.9946	0.0558	1.0007	0.7875	0.9899	0.9978
		Modeled	0.9893	0.9970	0.2480	1.0009	0.9243	0.9990	0.9993
4	FD	Normal	1.9538	1.9461	2.0000	1.9350	1.9631	1.9446	1.9360
		Low grade	1.9396	1.9257	2.0000	1.9152	1.9458	1.9230	1.9157
		Modeled	1.9850	1.9800	2.0000	1.9782	1.9862	1.9799	1.9786
5	Time Elapsed in Seconds	Normal	0.3205	2.4863	2.6805	76.4707	141.148	0.1826	0.3409
		Low grade	0.3285	2.5000	2.7020	76.3472	136.449	0.1704	0.3079
		Modeled	0.3288	2.5007	2.7004	76.8476	143.011	0.1699	0.3123

BS – BayesShrink, NS – NeighShrink, BF – Bilateral Filter, DCT – Discrete Curvelet Transform, TF – Trilateral Filter, VS –VisuShrink

V. CONCLUSION AND FUTURE WORK

In this paper the fractional Brownian motion noise is generated by using random midpoint displacement algorithm. The generated fBm noise with H = 0.3 and H = 0.7 is added to various brain MRI images. The performance of different noise reduction techniques for fBm noise is analyzed. The parameters, namely PSNR, SSIM, IEF, FD and time elapsed are compared. The performance of NeighShrink, VisuShrink (soft) and discrete curvelet transform are slightly better than other techniques in terms PSNR; moreover the fBm noise is not completely removed. The time elapsed for curvelet transform is higher than other noise reduction

techniques. Results of the analysis presented in this paper indicate the need for further research in the study of performance verses removal of fBm noise and computational complexity.

REFERENCES

[1]. Mandelbrot B.B. and Van Ness J.W., 1968,"Fractional Brownian motion, fractional noises and applications", SIAM Rev., Vol.10, pp. 422-437.
[2]. Mandelbrot B.B., 1983, "The Fractal Geometry of Nature", Freeman, San Francisco, CA.
[3]. David L Donoho and IainM.Johnstone, December 1995,"Adapting to unknown smoothness via wavelet shrinkage," Journal of the American Statistical Assoc., Vol. 90, No.432,pp.1200–1224.
[4]. D. L. Donoho and I. M. Johnstone, 1994, "Ideal spatial adaptation via wavelet shrinkage," Biometrika, Vol. 81, pp. 425–455.
[5]. Iain M.Johnstone and David L Donoho, 1995,"Wavelet shrinkage: Asymptopia?," J. R. Stat. Soc. B, Ser. B, vol. 57, no. 2, pp. 301–369.
[6]. C. Tomasi _ R. Manduchi, 1998, "Bilateral Filtering for Gray and Color Images",Proceedings of the 1998 IEEE International Conference on Computer Vision, Bombay, India.
[7]. Wilbur C. K. Wong, Albert C. S. Chung and Simon C. H. Yu, 2004, "Trilateral Filtering for Biomedical Images", IEEE International Symposium on Biomedical Imaging: from Nano toMacro, April 2004 (ISBI'04), Arlington, VA, USA, pp. 820 – 823, April 15-18.
[8]. Donoho D L and Johnstone IM, 1994, Ideal spatial adaptation by wavelet shrinkage', Biometrika, vol.81, no.3, pp. 425-455.
[9]. S. Grace Chang, Bin Yu and Martin Vetterli, September 2000, "Adaptive Wavelet Thresholding for Image Denoising and Compression," IEEE Transactions on Image Processing, Vol. 9, No. 9.
[10]. Jean-Luc Starck, Emmanuel J. Candès, and David L. Donoho, June 2002, "The Curvelet Transform for Image Denoising", IEEE Transactions on Image Processing, Vol. 11, No. 6.
[11]. G.Y.Chen, T.D.Bui and A.Krzyzak, 2004, "Image Denoising Using Neighbouring wavelet Coefficients", ICASSP, pp 917-920.
[12]. Yaglom A.M., 1986, "Correlation Theory of Stationary and Related Random Functions", New York: Springer – Verlag.
[13]. Patrick Flandrin, March 1992, "Wavelet analysis and synthesis of Fractional Brownian Motion", IEEE Trans. on Information Theory, vol.38, No. 2, pp.910-917.
[14]. Falconer K., 1990, "Fractal Geometry", Chichester: J.Wiley and Sons.
[15]. Ton Dieker, 2004, "Simulation of fractional Brownian motion".
[16]. Sellan F. and Meyer Y., 1996, "The Wavelet-Based Synthesis for Fractional Brownian Motion", Applied and Computational Harmonic Analysis, No.3, pp.377-383.
[17]. Penttinen A and Virtamo J, 2000, Thesis on "Simulation of Two-dimensional Fractional Brownian Motion".
[18]. S.Vanitha, R.Rajeswari and D.Ebenezer, March 2015, "A Novel Method to Model Brain Tumor using Wavelet Transform and Fractal Parameters", Australian Journal of Basic andApplied Sciences, 9(5), Pages: 418 – 423.